

## Supporting Information

### **Gel Electrolyte Interdigitation Enables Stable High Areal Capacity Cycling of 3D Zn Electrode**

*Yuan Shang,<sup>a</sup> Ravindra Kokate,<sup>a</sup> Patrick Tung,<sup>b</sup> Haoyin Zhong,<sup>c</sup> Erlantz Lizundia,<sup>d,e</sup> Francisco J Trujillo,<sup>a</sup> Priyank Kumar,<sup>a</sup> Dipan Kundu<sup>a\*</sup>*

<sup>a</sup> *School of Chemical Engineering, UNSW Sydney, Kensington, NSW 2052, Australia*

<sup>b</sup> *Research Technology Services (ResTech), UNSW Sydney, Kensington, NSW 2052, Australia*

<sup>c</sup> *Department of Materials Science and Engineering, National University of Singapore, 117575, Singapore*

<sup>d</sup> *Life Cycle Thinking Group, Department of Graphic Design and Engineering Projects, Faculty of Engineering in Bilbao, University of the Basque Country (UPV/EHU), 48013 Bilbao, Spain*

<sup>e</sup> *BCMaterials, Basque Center for Materials, Applications and Nanostructures, UPV/EHU Science Park, 48940 Leioa, Spain*

*\*Corresponding author. Email: [d.kundu@unsw.edu.au](mailto:d.kundu@unsw.edu.au)*

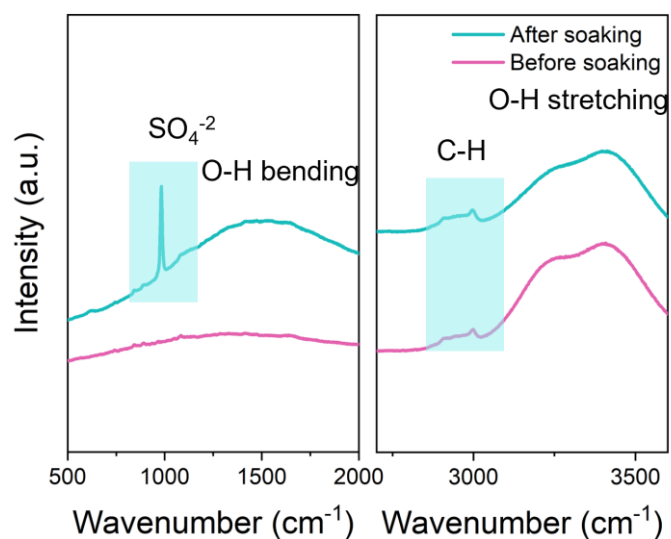


**Figure S1.** The Raman spectra of agarose hydrogel before and after soaking in 3M ZnSO<sub>4</sub> electrolyte.

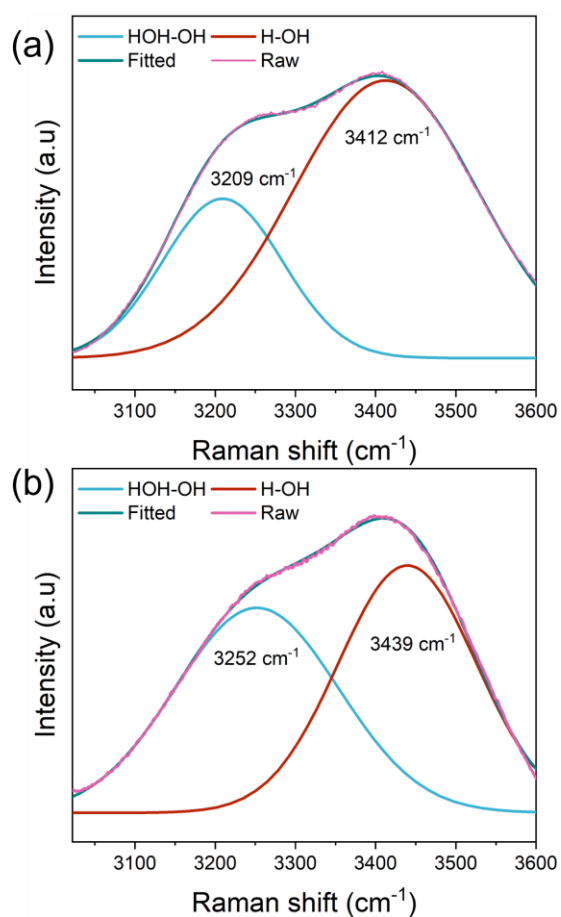


**Figure S2.** The enlarged Raman spectra of O-H stretch vibration for agarose hydrogel (a) before and (b) after soaking in 3M ZnSO<sub>4</sub> electrolyte.

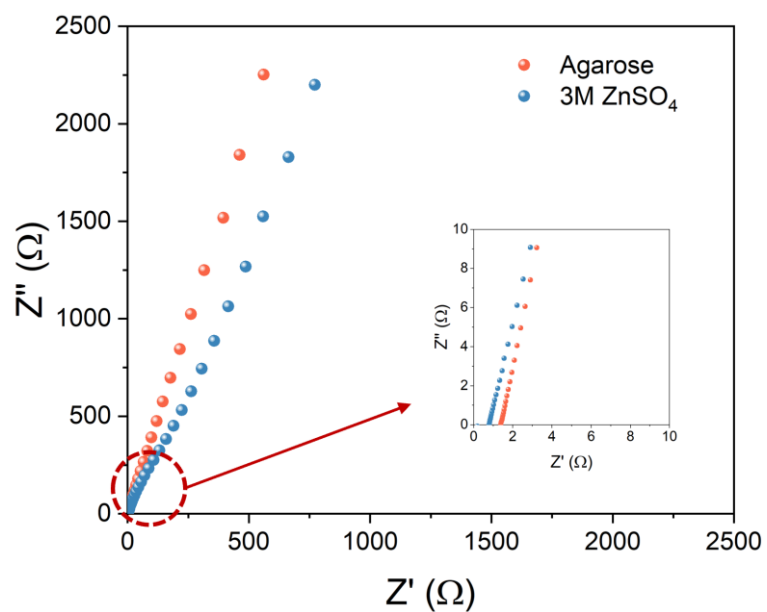


**Figure S3.** The Nyquist plot of agarose hydrogel electrolyte and 3M ZnSO<sub>4</sub> electrolyte obtained by Ti-Ti symmetric configuration.

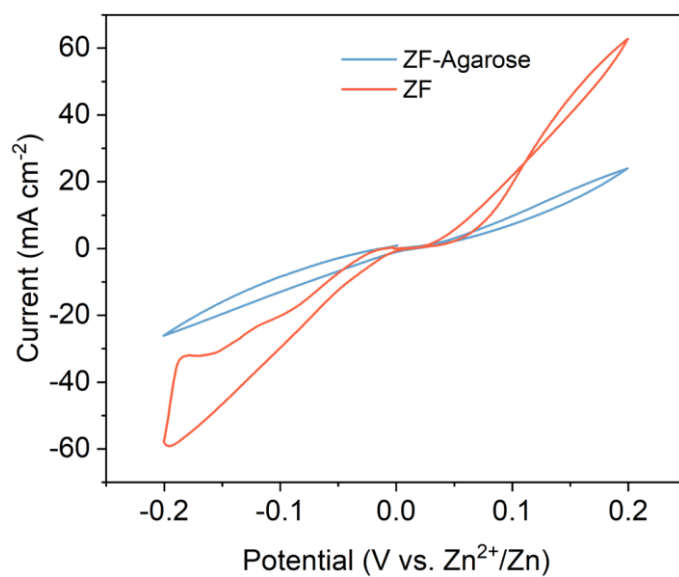


**Figure S4.** The CV profiles for ZF-Agarose and ZF electrode.

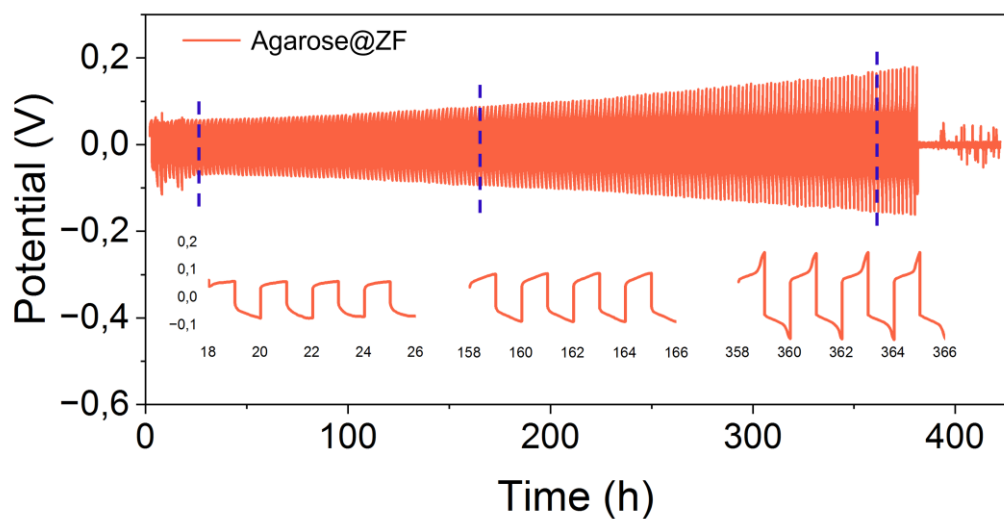


**Figure S5.** The long-term performance evaluation for Agarose@ZF electrode in symmetric configuration at 5 mA- 5 mAh cm<sup>-2</sup>.

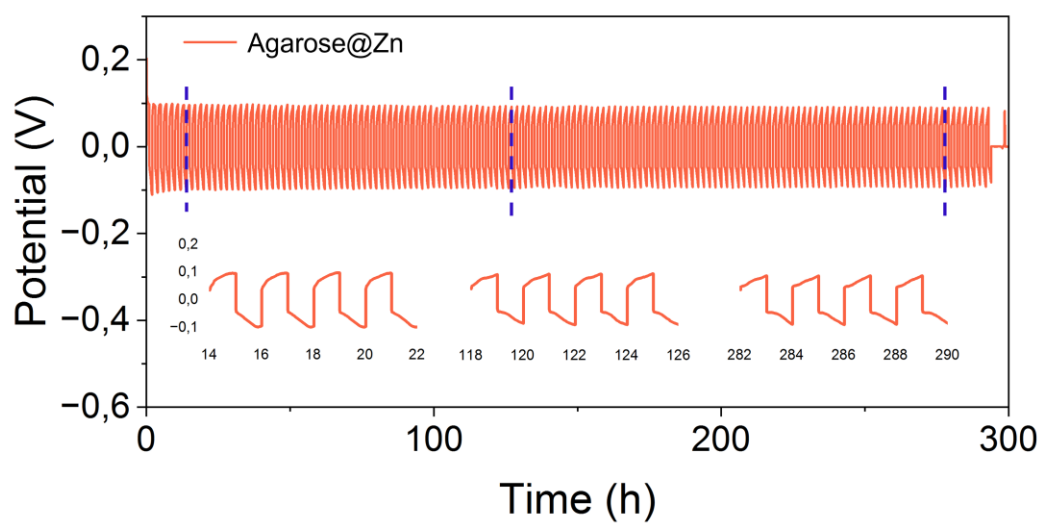


**Figure S6.** The long-term performance evaluation for Agarose@Zn electrode in symmetric configuration at 5 mA- 5 mAh cm<sup>-2</sup>.

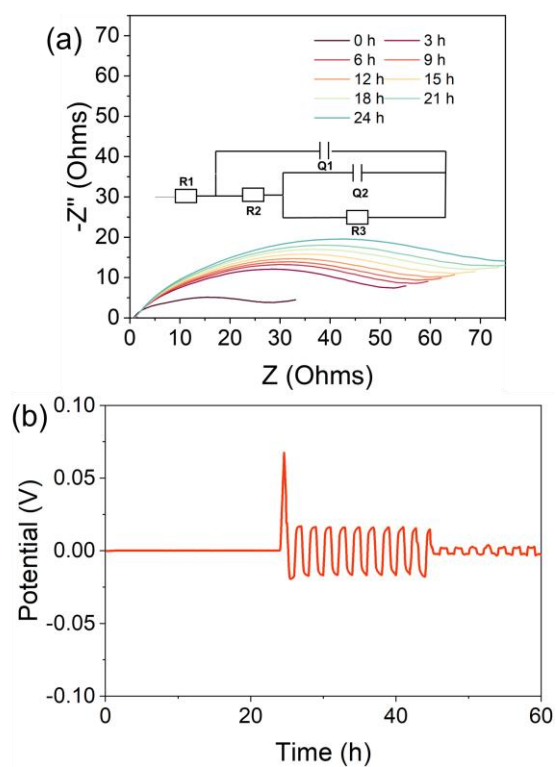


**Figure S7.** (a) The impedance evolution of ZF electrode during resting and (b) subsequent voltage profile when cycling at 2 mA- 2 mAh cm<sup>-2</sup>.

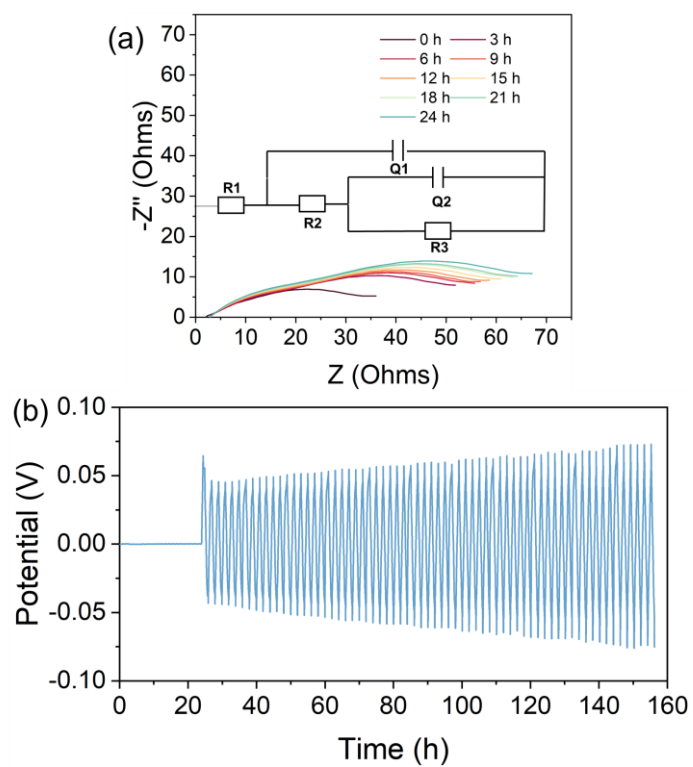


**Figure S8.** (a) The impedance evolution of ZF-Agarose electrode during resting and (b) subsequent voltage profile when cycling at 2 mA- 2 mAh cm<sup>-2</sup>. The inset in (a) shows the equivalent circuit model used to fit the impedance data. Further information is provided in the experimental details.

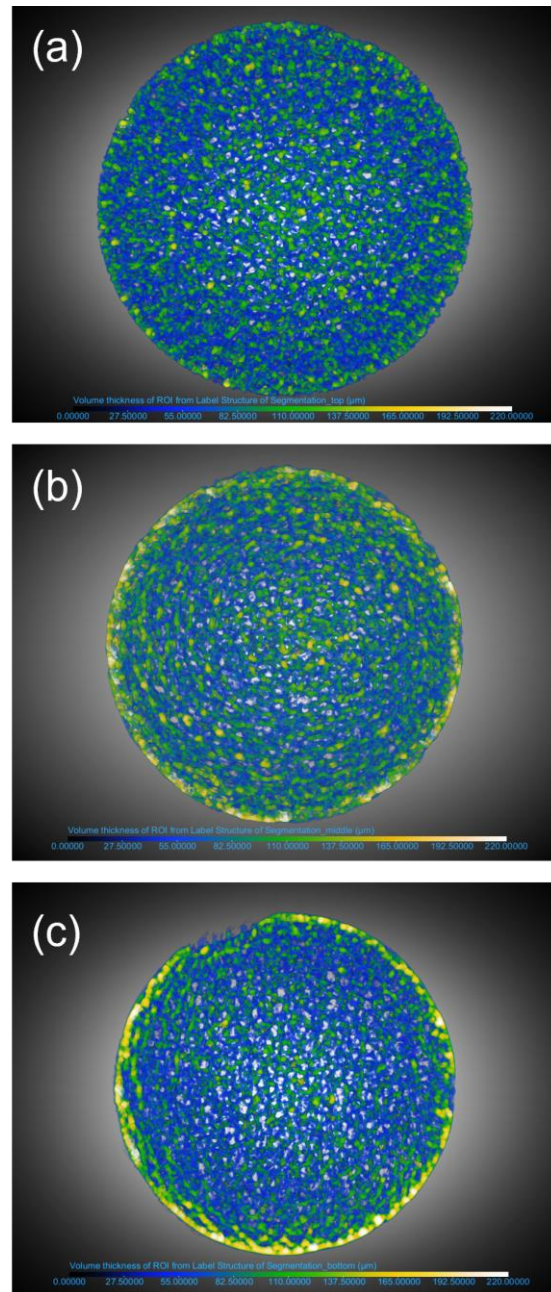


**Figure S9.** The volume thickness distribution for (a) pristine ZF, (b) cycled ZF-Agarose and (c) cycled ZF electrode.

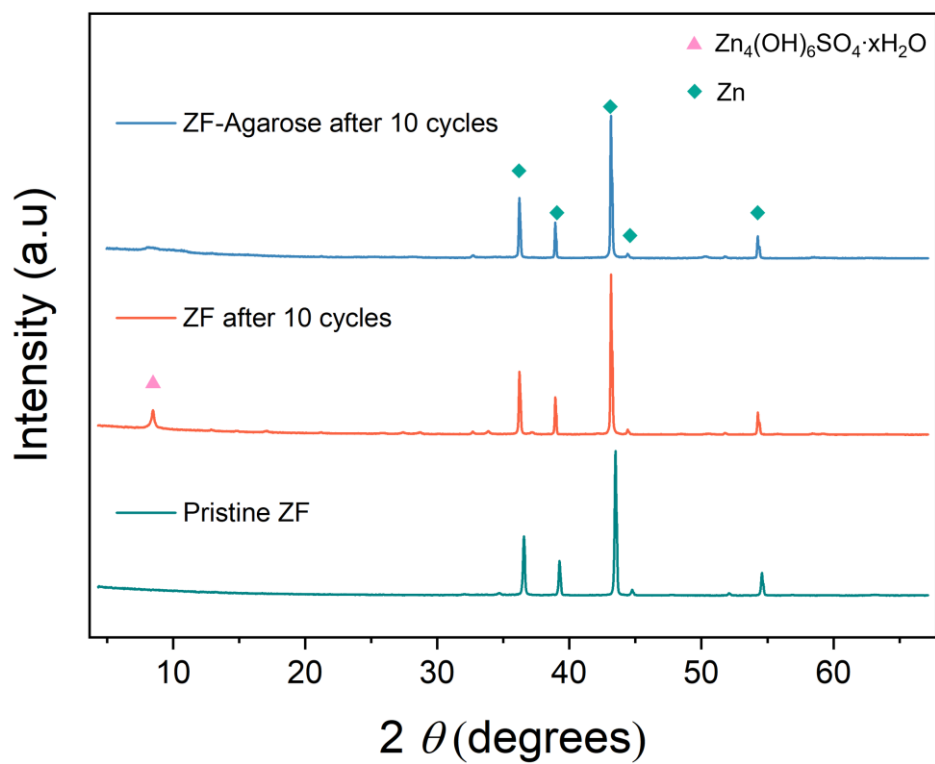


**Figure S10.** The XRD pattern of ZF and ZF-Agarose electrode after 10 cycles at 2 mA- 2 mAh cm<sup>-2</sup>

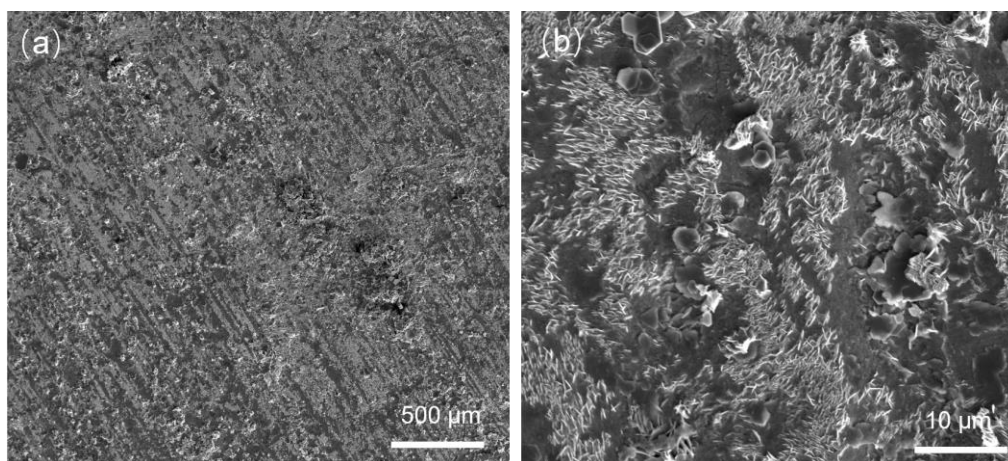


**Figure S11.** (a) The morphology of Agarose@Zn electrode with (b) higher magnification image after 10 cycles at 2 mA- 2 mAh cm<sup>-2</sup>



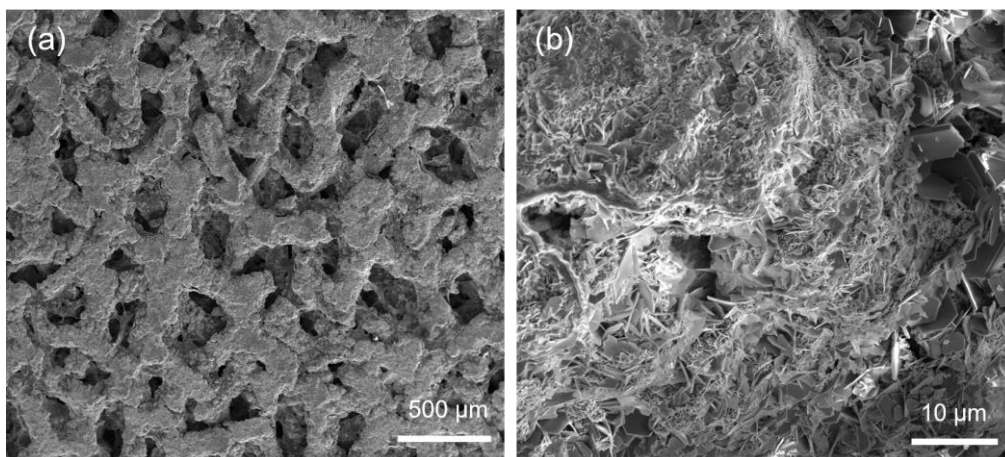


**Figure S12.** (a) The morphology of Agarose@ZF electrode with (b) higher magnification image after 10 cycles at 2 mA- 2 mAh cm<sup>-2</sup>

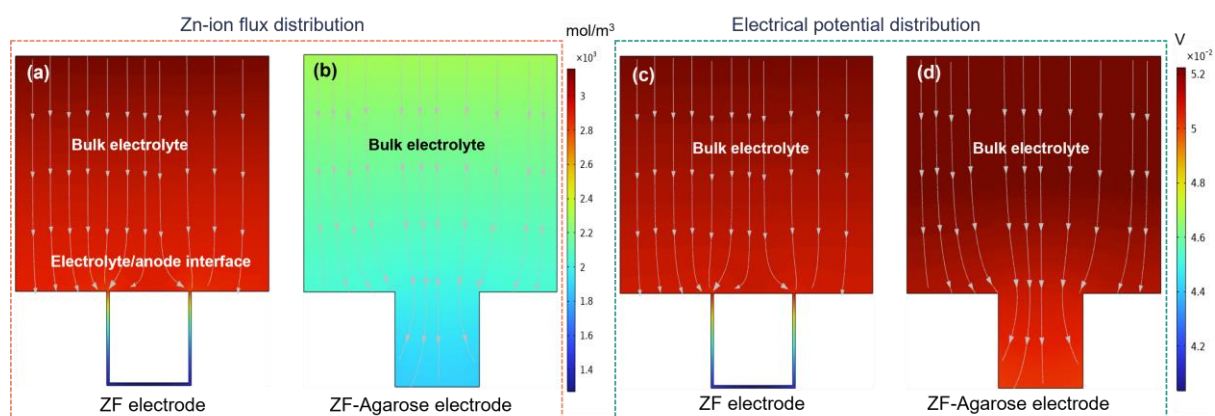


**Figure S13.** The 2D simulation model for Zn-ion flux distribution of (a) ZF and (b) ZF-Agarose electrode. The electrical potential distribution of (c) ZF and (d) ZF-Agarose electrodes.



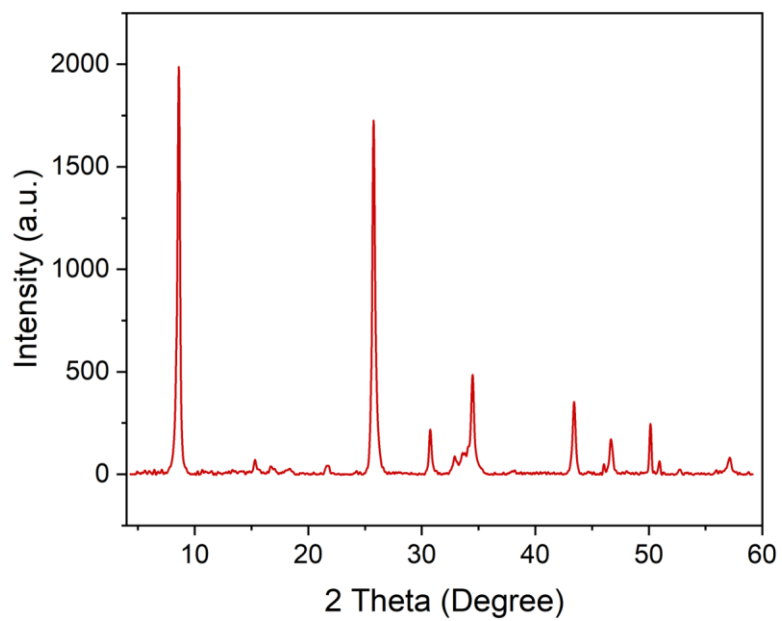


**Figure S14.** The XRD pattern of the ZVO cathode.

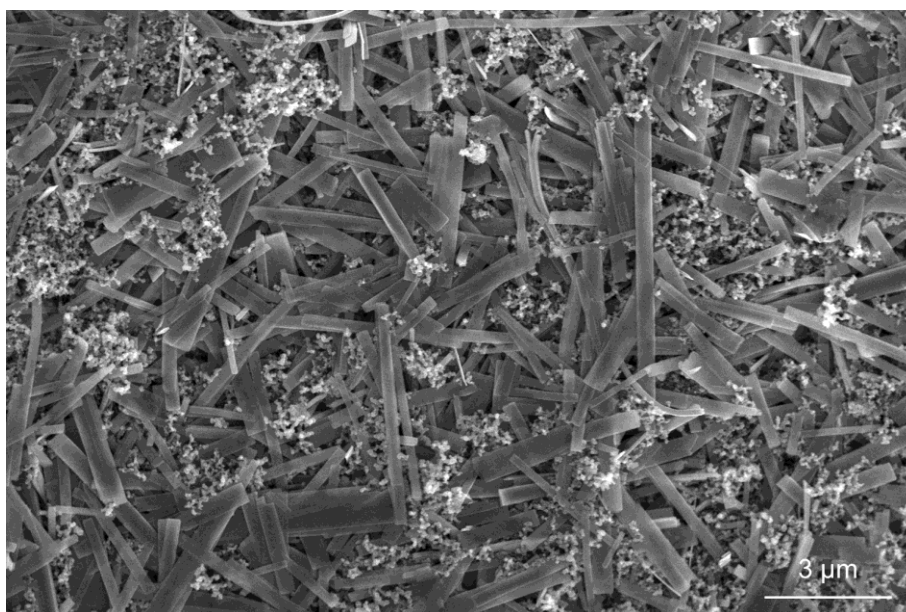


**Figure S15.** The SEM image of the ZVO cathode.

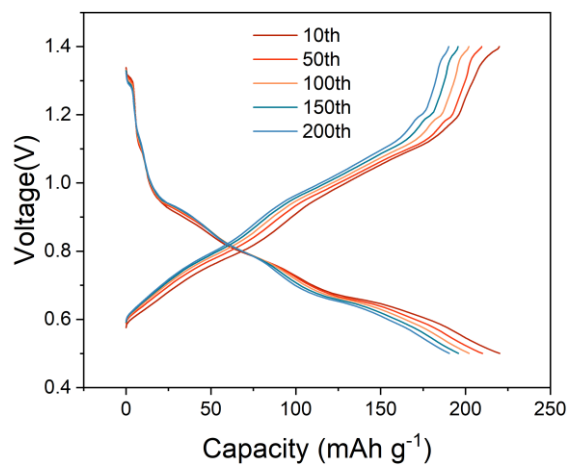


**Figure S16.** The corresponding voltage profile for ZVO//ZF-Agarose cell at 250 mA g<sup>-1</sup>.

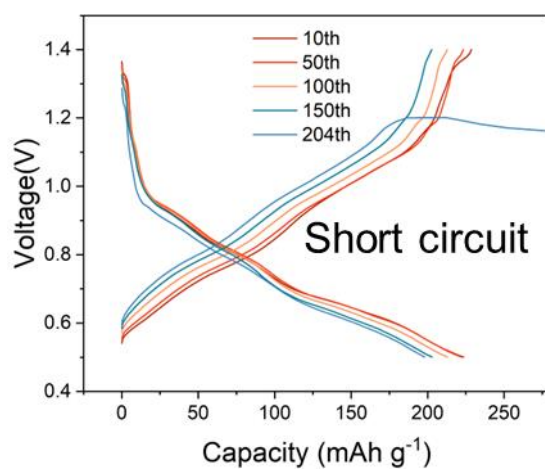


**Figure S17.** The corresponding voltage profile for ZVO//ZF cell at 250 mA g<sup>-1</sup>.